Particle Accelerators, 1996, Vol. 52, pp. 221–250
Reprints available directly from the publisher
Photocopying permitted by license only

ANALYTICAL FORMULAE FOR MAGNETIC MULTIPOLES

M. BASSETTI and C. BISCARI

INFN, Laboratori Nazionali di Frascati, Via E. Fermi 40, C.P. 13, 00044 Frascati, Italy

(Received 16 May 1995; in final form 1 February 1996)

Ironless distributions of currents creating pure multipolar fields are shown to exist. For cylindrical distributions the end-field potentials are analytically manageable. Fitting of real quadrupoles and solenoids are shown.

Keywords: Multipole potentials, analytical potentials, solenoids

1 INTRODUCTION

Magnetic multipole elements play an important role in particle accelerators. The main purpose of this paper is to obtain accurate values of the magnetic field (satisfying Maxwell's equations exactly) that can be used in theoretical computations. For real dipoles and quadrupoles, made of iron and coils, this is almost impossible because of construction errors, limited accuracy in magnetic design codes, and computing time. For this reason we decided to take into account only magnetic fields created by currents in vacuum.

We started with numerical calculations similar to those of Caspi.[1–3] Our work being purely speculative, current distributions were not linked to practical realization. On account of this conceptual freedom we discovered an interesting property. We simulated each pole of a quadrupole (see Figure 1) with a series of rectangular coils with the currents along the longitudinal sides distributed according to

$$I(\theta) = I_c \cos 2\theta \ .$$

Analysing the generated field we found as expected the presence of the odd harmonic terms starting from the dodecapole. Distributing the current of each pole on more coils did not result in a meaningful change and we therefore attributed

the higher harmonics to the coil shape. In fact the higher harmonics disappeared, changing the leaning of the head currents from the cords of the end circumferences to their arcs (see Figure 2).

Subtracting the currents of Figure 1 from those of Figure 2, the currents leaning on the longitudinal sides disappear and the results are coils of current leaning only on the cylinder basis, each made up of a cord and the corresponding piece of arc (see Figure 3). This arrangement of currents neutralizes the dodecapole and successive terms. We believe that the usual way of neutralizing the unwanted dodecapole of a normal quadrupole with chamfers on the quadrupole ends and the modification of the current arrangement in our model are equivalent.

Later on we discovered that these current arrangements are mathematically manageable. The conceptual path from the numerical to the analytical approach was very exciting. This paper will discuss only the analytical one. It will be shown that a mathematical treatment exists which holds for rectangular dipoles, quadrupoles, sextupoles, ..., and solenoids.

2 POTENTIAL AND FIELDS OF MULTIPOLES

2.1 Magnetic Potential

In the current-free region the magnetic field components of a multipole magnet can be obtained as a gradient of a scalar potential. Different mathematical approaches can be used to determine the potential. We will make use of the formulae developed previously.[1–4] We report in this section the most important developments. Using cylindrical coordinates, the potential corresponding to the harmonic m can be written as:

$$P_m(r, \phi, z) = \frac{r^m \sin m\phi}{m!} G_m(r, z) \ . \tag{1}$$

Replacing the factor $\sin m\phi$ by $\cos m\phi$ the potential represents skew elements. In the solenoidal case ($m = 0$) only the cosine choice is meaningful and the potential coincides directly with $G_m(r, z)$ (see Section 4). For the other cases, assuming:

$$G_m(r, z) = \sum_{p=0}^{\infty} G_{m2p}(z) r^{2p} \ , \tag{2}$$

the different terms $G_{m2p}(p > 0)$ are related to the function G_{m0} by the formula:

$$G_{m2p}(z) = (-1)^p \frac{m!}{4^p (m + p)! p!} \frac{d^{2p} G_{m0}}{dz^{2p}} \tag{3}$$

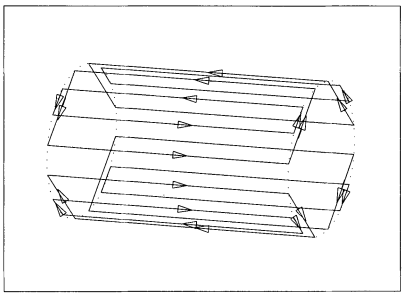

FIGURE 1: Coil network generating quadrupolar field plus odd harmonics.

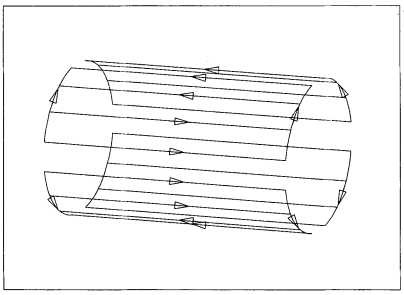

FIGURE 2: Coil network generating pure quadrupolar field.

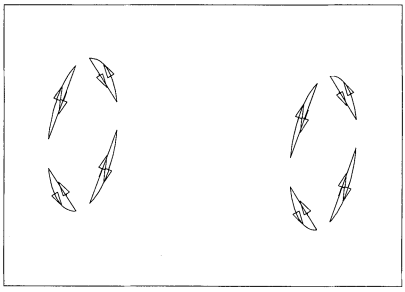

FIGURE 3: Coil network generating high harmonic terms.

and the potential for a single harmonic becomes:

$$P_m(r, \phi, z) = \frac{r^m \sin m\phi}{m!} \left\{ G_{m0}(z) + G_{m2}(z) r^2 + G_{m4}(z) r^4 + \ldots \right\} . \quad (4)$$

Let us emphasize that:

(i) The potential is a 2D potential times a function $G(r, z)$, and the dependence on ϕ is the same as the 2D solution.

(ii) Once m is fixed, all the potential is deducible from the function $G_{m0}(z)$.

(iii) The order of the harmonic m is also the lowest power of r. This ensures that if a potential can be written as:

$$P_m(r, \phi, z) = \sin m\phi \; Q(r, z) \tag{5}$$

the lowest power of r is also m, namely:

$$Q(r, z) = r^m \sum_{p=0}^{\infty} G_{m2p}(z) r^{2p} \; . \tag{6}$$

The potential in Equation (4) can be differentiated m times with respect to r at the point $r = 0$. The result, which will be useful in the following to deduce $G_{m0}(z)$, is:

$$\sin m\phi \; G_{m0}(z) = \left(\frac{\partial^m P_m(r, \phi, z)}{\partial r^m} \right)_{r=0} \; . \tag{7}$$

2.2 Magnetic Field

Since the scalar magnetic potential is just a mathematical tool, we define the magnetic field simply as its gradient, without the usual negative sign. The three field components in cylindrical coordinates are:

$$B_r(r, \phi, z) = \frac{\sin m\phi}{m!} \sum_{p=0}^{\infty} (m + 2p) G_{m2p}(z) \; r^{2p+m-1} \tag{8}$$

$$B_\phi(r, \phi, z) = \frac{\cos m\phi}{(m-1)!} \sum_{p=0}^{\infty} G_{m2p}(z) \; r^{2p+m-1} \tag{9}$$

$$B_z(r, \phi, z) = \frac{\sin m\phi}{m!} \sum_{p=0}^{\infty} G_{m2p+1}(z) \; r^{2p+m} \tag{10}$$

where by writing $G_{m2p+1}(z)$ we mean the derivative with respect to z of $G_{m2p}(z)$:

$$G_{m2p+1}(z) = \frac{dG_{m2p}(z)}{dz} \; . \tag{11}$$

From the transverse cylindrical components the Cartesian ones are simply obtained:

$$B_x = B_r \cos\phi - B_\phi \sin\phi \ , \tag{12}$$

$$B_y = B_r \sin\phi + B_\phi \cos\phi \ . \tag{13}$$

From the point of view of the magnetic field the adoption of a scalar or a vector potential is equivalent. Deduction of Equations (8)–(10) from a vector potential has been known since 1966.[5,6] We take these two references from Le Duff[7] where they are applied to understand the effect of the fringing fields of the insertion quadrupoles in DORIS.

3 CURRENT DISTRIBUTIONS

3.1 Current Distributions Generating Pure Multipole Potentials

While in previous works[2,3] the purpose is the computation of the potential starting from fixed current distributions, in this paper we ask the following question: Does a current distribution exist in vacuum that can realize a pure multipolar potential?

The answer is positive, as mentioned in the introduction. Figure 4 shows the cylindrical geometry of a current distribution which realizes a pure multipole of order m. The current $I(\theta)$ circulating on the two circumferences of the bases is:

$$I(\theta) = I_c \sin m\theta \ . \tag{14}$$

On the lateral surface of the cylinder the linear current density $J(A\ m^{-1})$ must be such that:

$$J(\theta) R d\theta = I(\theta + d\theta) - I(\theta) \ , \tag{15}$$

from which:

$$J(\theta) = \frac{1}{R}\frac{dI(\theta)}{d\theta} = \frac{mI_c}{R}\cos m\theta \ . \tag{16}$$

To simplify the problem we consider a network made of a finite number of current wires instead of the continuous distribution. The final result will be obtained by a limit process. Let us consider Figure 5.

We have N wires, leaning on the lateral surface S, separated by an angle

$$\Delta\theta = 2\pi/N \tag{17}$$

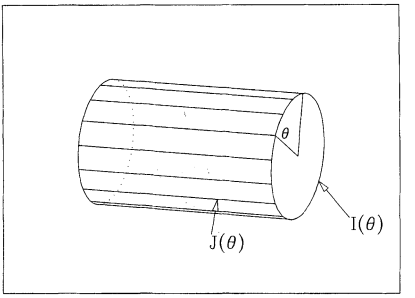

FIGURE 4: Current distribution generating a pure multipole.

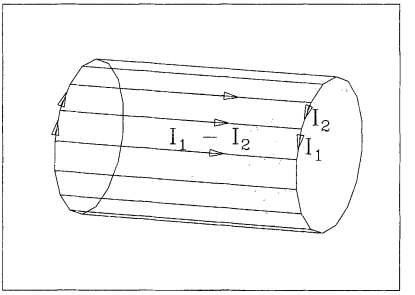

FIGURE 5: Net of current wires generating multipolar potentials.

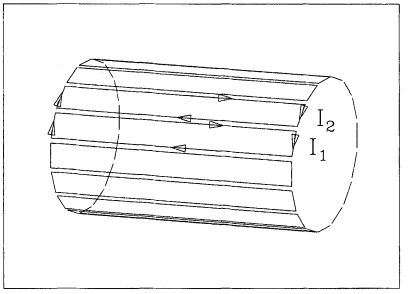

FIGURE 6: Net of coils generating multipolar potentials.

and N wires leaning on each of the two bases. The k-th current on the lateral surface is placed at an angle β_k:

$$\beta_k = k\Delta\theta \ . \tag{18}$$

Figure 6 shows how the current distribution of Figure 5 can be considered to be made of N rectangular coils adjacent to each other. The k-th coil is characterized by its average angle θ_k:

$$\theta_k = \left(k - \frac{1}{2}\right) \Delta\theta \tag{19}$$

and its current:

$$I(\theta_k) = I_c \sin m\theta_k \ . \tag{20}$$

The decomposition of the current distribution in a sum of coils is useful for the potential calculation. A coil carrying a current I induces at the point $Q_0(r, \phi, z)$ a potential:[8]

$$\Delta P = \frac{\mu_0 I}{4\pi} \Delta\omega \ , \tag{21}$$

where $\Delta\omega$ denotes the solid angle under which the coil is seen from $Q_0(r, \phi, z)$. Analogously to the network of currents we restrict the possible values of the Q_0 coordinate ϕ to N values, namely:

$$\phi_n = n\Delta\theta \ , \quad n = 1, \cdots, N \ . \tag{22}$$

The potential generated at a point $Q_0(r, \phi_n, z)$ by all the coils can be written as:

$$P_m(Q_0) = \frac{\mu_0 I_c}{4\pi} \sum_k \Delta\omega(\theta_k, \phi_n) \sin m\theta_k \ . \tag{23}$$

It can be observed that:

(i) for geometrical reasons the solid angle $\Delta\omega(\theta_k, \phi_n)$ depends only on the difference $\theta_k - \phi_n$. Through Equations (19) and (22) we obtain:

$$\theta_k - \phi_n = \left(k - n - \frac{1}{2}\right) \Delta\theta = \theta_{k-n} \tag{24}$$

and writing $\Delta\omega_{k-n}$ instead of $\Delta\omega(\theta_{k-n})$, the potential $P_m(Q_0)$ can be expressed as:

$$P_m(Q_0) = \frac{\mu_0 I_c}{4\pi} \sum_k \Delta\omega_{k-n} \sin\left(m\theta_{k-n} + m\phi_n\right) \ ; \tag{25}$$

(ii) for geometrical reasons as well, $\Delta\omega_{k-n}$ is an even function of θ_{k-n}, therefore inside $\sin(m\theta_{k-n} + m\phi_n)$ only the even terms in θ_{k-n} contribute to the sum. The potential can be rewritten:

$$P_m(Q_0) = \frac{\mu_0 I_c}{4\pi} \sin m\phi_n \sum_k \Delta\omega_{k-n} \cos m\theta_{k-n} \; ; \tag{26}$$

(iii) the dependence on n of the sum in Equation (26) is equivalent to a permutation of the N terms. Therefore the sum can be written:

$$P_m(Q_0) = \frac{\mu_0 I_c}{4\pi} \sin m\phi_n \sum_k \Delta\omega_k \cos m\theta_k \; . \tag{27}$$

Inside the sum, $\Delta\omega_k$ is now the solid angle under which the coil k is seen from the coordinate point $(r, 0, z)$ and not from the coordinate point (r, ϕ_n, z). At the limit of infinitesimal coils, $\Delta\omega_k$ becomes:

$$d\omega_k(Q_0) \to \frac{\partial\omega(\theta)}{\partial\theta} d\theta \tag{28}$$

and the potential, writing explicitly the dependence on the coordinates, is:

$$P_m(r, \phi, z) = \frac{\mu_0 I_c}{4\pi} \sin m\phi \int_0^{2\pi} \frac{\partial\omega(r, \theta, z)}{\partial\theta} \cos m\theta d\theta \; . \tag{29}$$

The potential depends on ϕ only through the factor $\sin m\phi$ and this guarantees that it corresponds to a pure multipole according to Equations (5) and (6).

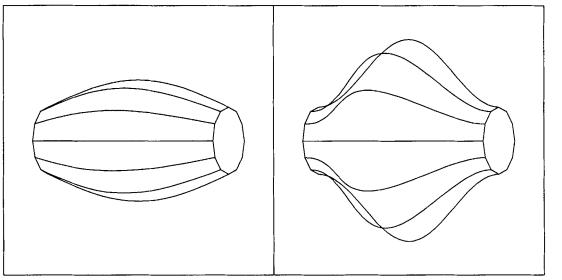

FIGURE 7: Cylindrical geometries with dependence on z generating multipole potential.

From the results, we observe that they are consequences only of the invariance under rotation of the cylindrical geometry, so we can extend the results to any surface S invariant under rotation around the z axis.

The surface S is completely defined by a curve $R(z)(-Z_L < z < Z_L)$. Figure 7 shows two examples with sinusoidal $R(z)$ functions. The current density $J(\theta)$ of Equation (16) in this case depends also on z according to:

$$J(z, \theta) = \frac{m I_c}{R(z)} \cos m\theta \ . \tag{30}$$

3.2 Current Distributions Generating Analytical Potentials

We demonstrate that the function $G_{m0}(z)$ (Equation (7)) can be expressed analytically if the surface S coincides with the lateral boundary of a cylinder of radius R.

According to the considerations of the previous section we need to compute the solid angle $d\omega(Q_0)$ under which an infinitesimal region on the cylinder placed around a point $Q(R, \theta, Z)$ is seen from a point $Q_0(r, 0, z)$. We can write:

$$d\omega(Q_0) = \frac{dS}{s^2} \cos\delta \tag{31}$$

where dS is the infinitesimal surface around $Q(R, 0, Z)$ (see Figure 8), s the distance between Q and Q_0, and δ the angle between QQ_0 and the normal to the cylindrical surface at the point Q. The surface element on the cylinder is:

$$dS = R\, d\theta\, dZ \ . \tag{32}$$

Let us now introduce the point Q_p, projection of Q on the z axis.

The Cartesian coordinates of Q, Q_0 and Q_p are, respectively, $(R\cos\theta,\ R\sin\theta,\ Z)$, $(r, 0, z)$ and $(0, 0, Z)$. Naming $\mathbf{s}$ the vector joining Q_0 to Q (s its module), $\mathbf{R}$ the one joining Q_p to Q_0 (R its module) we obtain:

$$s = \sqrt{R^2 + r^2 - 2Rr\cos\theta + (Z - z)^2} \tag{33}$$

$$\cos\delta = \frac{\mathbf{s}\cdot\mathbf{R}}{s\,R} = \frac{R - r\cos\theta}{s} \tag{34}$$

and finally, substituting inside Equation (35):

$$d\omega(Q_0) = \frac{R - r\cos\theta}{s^3} R\, d\theta\, dZ \ . \tag{35}$$

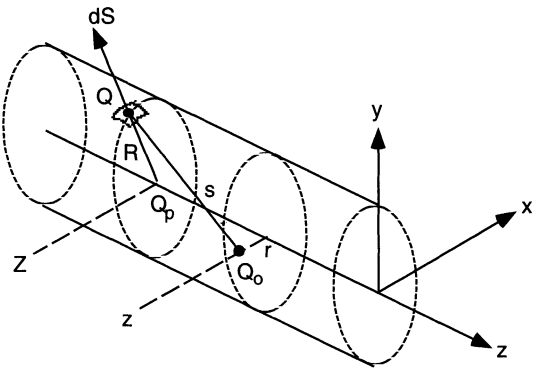

FIGURE 8: Sketch of the geometry used to determine the analytical potential.

Defining:

$$g(r,\theta) = \frac{R - r\cos\theta}{s^3} \tag{36}$$

we can write:

$$\frac{\partial\omega}{\partial\theta} = g(r,\theta)R\,dZ \tag{37}$$

and Equation (29) becomes:

$$P_m(r,\phi,z) = \frac{\mu_0 I_c R}{4\pi}\sin m\phi \int_{-Z_L}^{Z_L} dZ \int_0^{2\pi} g(r,\theta)\cos m\theta\, d\theta\ . \tag{38}$$

Comparison between Equations (38) and (7) gives for $G_{m0}(z)$:

$$G_{m0}(z) = \frac{\mu_0 I_c R}{4\pi} \int_{-Z_L}^{Z_L} dZ \int_0^{2\pi} \cos m\theta \left(\frac{\partial^m g(r,\theta)}{\partial r^m}\right)_{r=0} d\theta\ . \tag{39}$$

Instead of using the definite integral on Z it is convenient to use the indefinite one $G_{m0}(Z,z)$:

$$G_{m0}(Z,z) = \frac{\mu_0 I_c R}{4\pi} \int dZ \int_0^{2\pi} \cos m\theta \left(\frac{\partial^m g(r,\theta)}{\partial r^m}\right)_{r=0} d\theta \tag{40}$$

from which $G_{m0}(z)$ is:

$$G_{m0}(z) = G_{m0}(Z_L, z) - G_{m0}(-Z_L, z) \ . \tag{41}$$

The derivatives with respect to r and the integration on θ appearing in Equation (40) are performed in the first part of Appendix A and the integration on Z in the second part. Defining:

$$t = Z - z \tag{42}$$

$$A(t) = \sqrt{R^2 + t^2} \tag{43}$$

$$f_h(t) = \left(\frac{t}{A}\right)^h \qquad (h = 0, 1, \cdots \infty) \tag{44}$$

the final result is:

$$G_{m0}(t) = \mu_0 I_c \frac{(2m-1)!}{R^m 4^m (m-1)!} \sum_{k=0}^{m} (-1)^k \frac{m+k+1}{2k+1} \binom{m}{k} f_{2k+1}(t) \ . \tag{45}$$

This formula is valid only for $m > 0$.

3.3 Computation of High-order Terms of the Field

The derivation of the high-order terms of the field transverse components needs the even order derivatives on the function $G_{m0}(z)$ (Equation (45)) where the $f_{2k+1}(t)$ appear. The even differentiation with respect to z is equivalent to the one with respect to t (see Equation (42)); the second-order derivative with respect to t of the f_{2k+1} is performed in Appendix B. Substituting in Equation (B.8) the index h with $2k+1$ we can write:

$$\frac{\partial^2 f_{2k+1}}{\partial t^2} = \frac{1}{R^2}\Big[(4k^2+2k) f_{2k-1} - (12k^2+12k+3) f_{2k+1} + (12k^2+18k+6) f_{2k+3} - (4k^2+8k+3) f_{2k+5}\Big] \ . \tag{46}$$

The second-order derivative of f_{2k+1} is a linear combination of functions f_{2k-1}, f_{2k+1}, f_{2k+3}, f_{2k+5}: it introduces f_{2k-1}. Whatever the odd initial value of $2k+1$ is, by taking successive derivatives, we end up with f_1. At this point, applying Equation (46) we can see that no terms lower than f_1 are introduced:

$$\frac{\partial^2 f_1(t)}{\partial t^2} = \frac{-3f_1(t) + 6f_3(t) - 3f_5(t)}{R^2} . \tag{47}$$

Equation (46) suggests the definition of a matrix **M** associated with the second derivative. Only odd rows and columns of **M** must be considered and we can define:

$$\begin{aligned} M_{2k-1,2k+1} &= 4k^2 + 2k \\ M_{2k+1,2k+1} &= -(12k^2 + 12k + 3) \\ M_{2k+3,2k+1} &= 12k^2 + 18k + 6 \\ M_{2k+5,2k+1} &= -(4k^2 + 8k + 3) . \end{aligned} \tag{48}$$

The sum of the elements of any column of **M** vanishes. Since, according to Equation (44) asymptotically every f_{2k+1} is $+1$ at $+\infty$ and -1 at $-\infty$, all the even derivatives of f_{2k+1} vanish for $t \to \infty$. Table 1 shows the first elements of **M**.

TABLE 1: Matrix **M**.

n	M n,1	M n,3	M n,5	M n,7	M n,9	M n,11	M n,13	M n,15	M n,17	M n,19	M n,21	M n,23
1	- 3	6	0	0	0	0	0	0	0	0	0	0
3	6	- 27	20	0	0	0	0	0	0	0	0	0
5	- 3	36	- 75	42	0	0	0	0	0	0	0	0
7	0	- 15	90	- 147	72	0	0	0	0	0	0	0
9	0	0	- 35	168	- 243	110	0	0	0	0	0	0
11	0	0	0	- 63	270	- 363	156	0	0	0	0	0
13	0	0	0	0	- 99	396	- 507	210	0	0	0	0
15	0	0	0	0	0	- 143	546	- 675	272	0	0	0
17	0	0	0	0	0	0	- 195	720	- 867	342	0	0
19	0	0	0	0	0	0	0	- 255	918	- 1083	420	0
21	0	0	0	0	0	0	0	0	- 323	1140	- 1323	506

M does not depend on the multipole order m and on the order of derivation p. In the first column $-3, 6, -3$ are the coefficients of the second derivative of f_1, in the second column $6, -27, 36, -15$ those of the second derivative of f_3 and so on.

Let us now introduce a vector $\mathbf{F}_{m0}$, associated with the function G_{m0} (see Equation (45)) with components:

$$\mathbf{F}_{m,0,2k+1} = (-1)^k \frac{(2m-1)!}{4^m(m-1)!} \frac{m+k+1}{2k+1} \binom{m}{k} . \tag{49}$$

Functions G_{m2p} [defined in Equation (3)] are proportional to the even derivatives of G_{m0}. So, introducing the matrix $\mathbf{M}$, associated with the second derivative of functions f_{2k+1}, we can associate with each G_{m2p} the vectors $\mathbf{F}_{m2p}$:

$$\mathbf{F}_{m2p} = \frac{(-1)^p m!}{4^p(m+p)!p!} \mathbf{M}^p \mathbf{F}_{m0} \tag{50}$$

with components:

$$F_{m,2p,2k+1} = \frac{(-1)^p m!}{4^p(m+p)!p!} (\mathbf{M}^p \mathbf{F}_{m0})_{2k+1} . \tag{51}$$

All $F_{m,2p,2k+1}$ are zero for $k > m + 2p$, so that Equation (3) can be rewritten:

$$G_{m2p}(t) = \frac{\mu_0 I_c}{R^{m+2p}} \sum_{k=0}^{\infty} F_{m,2p,2k+1} f_{2k+1}(t) . \tag{52}$$

Finally, passing from the indefinite to the finite integration from $-Z_L$ to Z_L:

$$G_{m2p}(z) = \frac{\mu_0 I_c}{R^{m+2p}} \sum_{k=0}^{\infty} F_{m,2p,2k+1} [f_{2k+1}(Z_L - z) + f_{2k+1}(Z_L + z)] . \tag{53}$$

We notice that while $G_{m2p}(t)$ is an odd function, $G_{m2p}(z)$ is an even function.

To obtain $B_z(r, \phi, z)$ each f_{2k+1} must be differentiated once. In Appendix B we show that the derivative of $f_{2k+1}(t)$, that we call $g_{2k+1}(t)$ can be written:

$$g_{2k+1}(t) = \frac{df_{2k+1}(t)}{dt} = \frac{(2k+1)R^2}{A^3} f_{2k}(t) . \tag{54}$$

From the above equation and definition (44) $f_{2k+1}(t)$ and $g_{2k+1}(t)$ have opposite parities. Recalling Equations (11) and (53) we can write:

$$G_{m2p+1}(z) = \frac{\mu_0 I_c}{R^{m+2p}} \sum_{k=0}^{\infty} F_{m,2p,2k+1} [g_{2k+1}(Z_L + z) - g_{2k+1}(Z_L - z)] . \tag{55}$$

So $G_{m2p+1}(z)$ is odd.

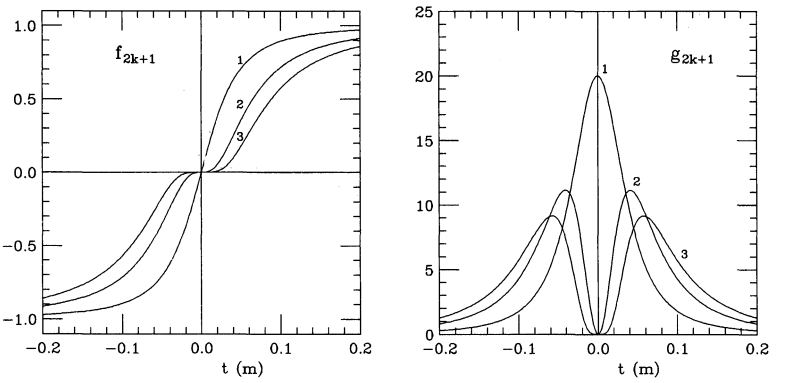

FIGURE 9: Functions $f_{2k+1}(t)$ and $g_{2k+1}(t)$ for $k = 1, 2, 3$.

From the above considerations the fundamental role of the odd functions $f_{2k+1}(t)$ and their derivatives $g_{2k+1}(t)$ appears. The behaviour of the functions $f_{2k-1}(t)$ and $g_{2k+1}(t)$ is shown in Figure 9 for $k = 1, 2, 3$.

Tables containing the coefficients $F_{m,2p,2k+1}$ for the dipole and the quadrupole are reported subsequently as an example which shows the spectrum of functions $f_{2k+1}(t)$ for the functions $G_{m2p}(t)$ and the spectrum of functions $g_{2k+1}(t)$ for the functions $G_{m2p+1}(t)$.

In Table 2 the first column ($p = 0$) contains the coefficients of f_1 and f_3 in $G_{10}(z)$ except for the factor $\mu_0 I_c/R$. The second column the coefficients of f_1, f_3 and f_5 in $G_{12}(z)$ except for the factor $\mu_0 I_c/R^3$, etc. Passing from the dipole to the quadrupole the spectrum of f_{2k+1} inside $G_{m0}(z)$ (see first column in Tables 2 and 3) adds f_5.

TABLE 2: Dipole coefficients $F_{1,2p,2k+1}$.

k	$p = 0$	$p = 1$	$p = 2$	$p = 3$
1	0.50	0.37500	0.35156250	0.34179687500
2	−0.25	−1.21875	−2.55859375	4.31518554685
3	0.00	1.31250	6.79687500	20.04638671850
4	0.00	−0.46875	−8.55468750	−47.53540039050
5	0.00	0.00000	5.19531250	64.01855468750
6	0.00	0.00000	−1.23046875	−49.75708007850
7	0.00	0.00000	0.00000000	20.86669921850
8	0.00	0.00000	0.00000000	3.66577148435

TABLE 3: Quadrupole coefficients $F_{2,2p,2k+1}$.

k	$p=0$	$p=1$	$p=2$	$p=3$
0	1.125	0.78125	0.7177734375	0.692138671875
1	−1.000	−3.43750	−6.5625000000	−10.510253906250
2	0.375	5.62500	22.4560546875	59.031738281250
3	0.000	−4.06250	−38.5546875000	172.727050781250
4	0.000	1.09375	35.7861328125	297.568359375000
5	0.000	0.00000	−17.2265625000	314.538574218750
6	0.000	0.00000	3.3837890625	201.335449218750
7	0.000	0.00000	0.0000000000	−71.849121093750
8	0.000	0.00000	0.0000000000	10.997314453125

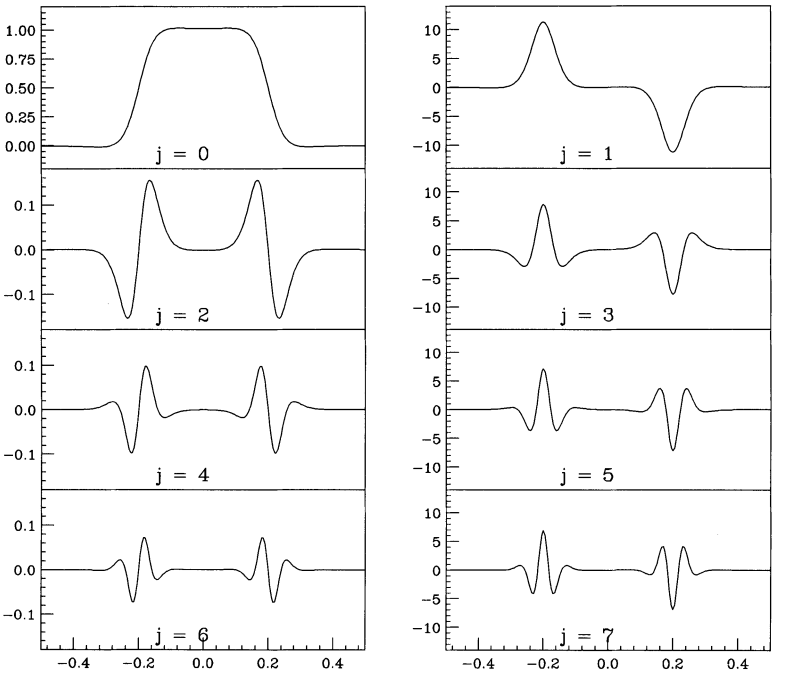

FIGURE 10: Functions $G_{2j}(j = 0, 1, \cdots, 7)$ for a quadrupole with $Z_L = 0.2$ m and $R = 0.1$ m. The factor $\mu_0 I_c / R^{2p+2}$ has been omitted and therefore the vertical scales are dimensionless for the even terms and (m^{-1}) for the odd ones.

Figure 10 represents an example of the functions G_{2j} up to the 7th order. According to Equations (8)–(10), G_{20} is proportional to the basic focusing component of the fields, G_{21} to the first term of the longitudinal component, G_{22} to the pseudo-octupole component of the transverse fields, G_{23} to the second term of B_z and so on.

4 SOLENOIDAL CASES

4.1 The $m = 0$ Case

For $m = 0$ only the case with $\cos m\phi$ is meaningful. The potential is:

$$P_0(r, z) = \left\{ G_{00}(z) + G_{02}(z)r^2 + G_{04}(z)r^4 + \cdots \right\} \tag{56}$$

and the components of the magnetic field (B_ϕ is always vanishing):

$$B_r(r, z) = 2 \sum_{p=1}^{\infty} p\, G_{02p}(z) r^{2p-1} \tag{57}$$

$$B_z(r, z) = \sum_{p=0}^{\infty} G_{02p+1}(z) r^{2p} \,. \tag{58}$$

The first term in B_z is proportional to $G_{01}(z)$, and in B_r proportional to $G_{02}(z)$.

Using the scheme of N coils lying on the surface S (see Figure 5) the solenoidal case presents unusual peculiarities. Since $m = 0$, the current running through adjacent coils (see Figure 6) is always the same, the two currents of adjacent meridians compensate each other exactly and the resulting scheme becomes two end coils (TEC) with opposite currents. Nevertheless the interpretation of the current network as sum of N rectangular coils remains valid.

It could be remarked that the TEC case could be obtained simply by superposition of two coils, but in fact it is useful in our analysis for two reasons: first it is the natural extrapolation to $m = 0$ of the series $m = 2$ (quadrupole), $m = 1$ (dipole), and second its solution is strictly linked to the solenoidal case (see Section 4.2).

At the limit of a continuous distribution of currents adopting Equation (39) with $m = 0$ and $r = 0$ we obtain $G_{00}(z)$:

$$G_{00}(z) = \frac{\mu_0 I_c}{4\pi} \int_{-Z_L}^{Z_L} dZ \int_0^{2\pi} \frac{R^2}{\sqrt{[R^2 + (Z - z)^2]^3}} d\theta \,. \tag{59}$$

The integration over θ gives simply a factor 2π and introducing the variable t, $G_{00}(z)$ becomes:

$$G_{00}(z) = \frac{\mu_0 I_c}{2} \int_{-Z_L - z}^{Z_L - z} \frac{R^2}{\sqrt{(R^2 + t^2)^3}} dt \ . \tag{60}$$

Finally:

$$G_{00}(z) = \frac{\mu_0 I_c}{2} [f_1(Z_L - z) + f_1(Z_L + z)] \ . \tag{61}$$

In $G_{00}(z)$ an odd f_{2k+1} appears, analogously to the cases with $m > 0$. The vector $\mathbf{F}_{00}$ components are now deduced from expression (61):

$$F_{0,0,1} = \frac{1}{2} \quad F_{0,0,2k+1} = 0 \quad k = 1, 2, \ldots \infty \ . \tag{62}$$

Using the vector $\mathbf{F}_{00}$ all the formulae from (50) to (55) can be applied. We report only the most meaningful ones:

$$F_{0,2p,2k+1} = \frac{(-1)^p}{4^p (p!)^2} (\mathbf{M}^p \mathbf{F}_{00})_{2k+1} \tag{63}$$

$$G_{02p}(z) = \frac{\mu_0 I_c}{R^{2p}} \sum_{k=0}^{\infty} F_{0,2p,2k+1} \ [f_{2k+1}(Z_L - z) + f_{2k+1}(Z_L + z)] \tag{64}$$

$$G_{02p+1}(z) = \frac{\mu_0 I_c}{R^{2p}} \sum_{k=0}^{\infty} F_{0,2p,2k+1} [-g_{2k+1}(Z_L - z) + g_{2k+1}(Z_L + z)] \ . \tag{65}$$

Choosing only the second term of (64) and (65) and putting $Z_L = 0$, i.e. placing the coil at the origin, we obtain the formulae for a single coil. We report for the sake of simplicity only $G_{c0}(z)$:

$$G_{c0}(z) = \frac{\mu_0 I_c}{2} f_1(z) \ . \tag{66}$$

We observe that the absence of the two limits of (61) changes the parity of $G_{c0}(z)$ with respect to $G_{00}(z)$.

A simple derivation of Equation (66) gives the longitudinal magnetic field on the axis of the coil:

$$B_z(z) = \frac{\mu_0 I_c}{2} \frac{R^2}{(R^2 + z^2)^{3/2}} \ . \tag{67}$$

TABLE 4: Coefficients $F_{0,2p,2k+1}$ corresponding to the Coil and TEC.

k	$p=0$	$p=1$	$p=2$	$p=3$
0	0.5	0.375	0.3515625	0.341796875
1	0.0	–0.750	–1.8750000	–3.417968750
2	0.0	0.375	3.5156250	12.509765625
3	0.0	0.000	–2.8125000	–22.695312500
4	0.0	0.000	0.8203125	22.080078125
5	0.0	0.000	0.0000000	–11.074218750
6	0.0	0.000	0.0000000	2.255859375

This formula could be obtained by Equation (5.14) of Jackson[9] and it is explicitly written in Amaldi.[10]

From (63) we deduce the table of coefficients $F_{0,2p,2k+1}$ valid for the Coil and the TEC cases. They are reported in Table 4.

4.2 Solenoid

The total current of the solenoid being I_S, the density function $J_S(Z)$ on its lateral surface is:

$$J_S(Z) = \frac{I_S}{2Z_L}[u(Z+Z_L) - u(Z-Z_L)] \,. \tag{68}$$

We can consider a solenoid as a set of coils uniformly covering the space between $-Z_L$ and Z_L. The potential on the axis (see Equation (66)) is:

$$G_{S0}(z) = \frac{\mu_0}{2} \int_{-\infty}^{\infty} J_S(Z) f_1(z-Z) dZ \,. \tag{69}$$

Integrating this expression with respect to z we obtain:

$$G_{S0}(z) = \frac{\mu_0 I_S}{2Z_L} \frac{\sqrt{R^2+(z+Z_L)^2} - \sqrt{R^2+(z-Z_L)^2}}{2} \tag{70}$$

and $G_{S1}(z)$ becomes:

$$G_{S1}(z) = \frac{\mu_0 I_S}{4Z_L}[f_1(z+Z_L) - f_1(z-Z_L)] \,. \tag{71}$$

By successive derivatives all $G_{S2p}(z)$ and $G_{S2p+1}(z)$ functions can be obtained, and remembering Equations (46),(54) we can deduce that any $G_{S2p+1}(z)$ is made up of f_{2k+1} and any $G_{S2p}(z)$, with the only exception of $G_{S0}(z)$, is made up of g_{2k+1}. To obtain the corresponding coefficients we first observe that $G_{S1}(z)$ (Equation (71)) and $G_{00}(z)$ relative to the TEC [Equation (61)] have the same behaviour, and we can write for $p = 0, 1, 2, \cdots$:

$$G_{S2p+1}(z) = \frac{dG_{S2p}(z)}{dz} = \frac{\mu_0 I_S}{2R^{2p}Z_L} \sum_{k=0}^{\infty} F_{0,2p,2k+1}[f_{2k+1}(z+Z_L) - f_{2k+1}(z-Z_L)] \tag{72}$$

and by derivation with respect to z:

$$\frac{d^2G_{S2p}(z)}{dz^2} = \frac{\mu_0 I_S}{2R^{2p}Z_L} \sum_{k=0}^{\infty} F_{0,2p,2k+1}[g_{2k+1}(z+Z_L) - g_{2k+1}(z-Z_L)] \,. \tag{73}$$

Using Equation (3) we deduce:

$$G_{S2p+2}(z) = (-1)^{p+1} \frac{1}{4^{p+1}(p+1)!2} \frac{d^{2p+2}G_{S0}}{dz^{2p+2}} = -\frac{1}{4(p+1)^2} \frac{d^2G_{S2p}(z)}{dz^2} \tag{74}$$

and Equation (73) can be rewritten:

$$G_{S2p+2}(z) = -\frac{1}{4(p+1)^2} \frac{\mu_0 I_S}{2R^{2p}Z_L} \sum_{k=0}^{\infty} F_{0,2p,2k+1}[g_{2k+1}(z+Z_L) - g_{2k+1}(z-Z_L)] \tag{75}$$

and introducing for simplicity new coefficients $D_{0,2p+2,2k+1}$ defined as:

$$D_{0,2p+2,2k+1} = -\frac{1}{4(p+1)^2} F_{0,2p,2k+1} \tag{76}$$

$$G_{S2p+2}(z) = \frac{\mu_0 I_S}{2R^{2p}Z_L} \sum_{k=0}^{\infty} D_{0,2p+2,2k+1}[g_{2k+1}(z+Z_L) - g_{2k+1}(z-Z_L)] \tag{77}$$

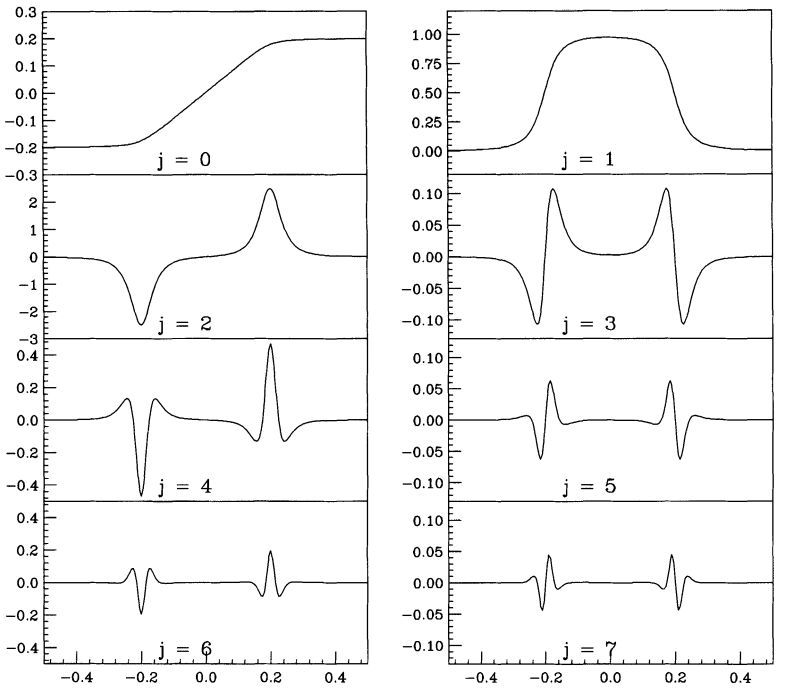

FIGURE 11: Functions $G_{Sj}(j = 0, 1, \cdots 7)$ for a solenoid with $Z_L = 0.2$ m and $R = 0.05$ m. They are plotted normalized to the factor $\mu_0 I_S/2R^n Z_L$ and therefore the vertical scales are dimensionless for odd j and (m^{-1}) for even j.

from which:

$$G_{S2p}(z)\frac{\mu_0 I_S}{2R^{2p-2}Z_L}\sum_{k=0}^{\infty} D_{0,2p,2k+1}[g_{2k+1}(z+Z_L) - g_{2k+1}(z-Z_L)] \quad (p>0)\,. \tag{78}$$

Let us summarize: the functions G_{S2p+1} are obtained with the coefficients $F_{0,2p,2k+1}$ reported in Table 4, while the functions G_{S2p} contain the modified coefficients $D_{0,2p,2k+1}$. The parity of the solenoidal function is opposite to that of the multipoles with $m > 0$.

Figure 11 represents an example of the functions $G_{Sj}(z)$ up to the 7th order for a solenoid with $Z_L = 0.2$ m and $R = 0.05$ m. The functions with odd j determine the longitudinal component of the field, those with even j determine the radial component. From the point of view of field components G_{S0} can be ignored.

5 FINAL CONSIDERATIONS

The formalism which describes the magnetic potential near the axis of a multipole, developed by Caspi[1–3] and Leleux[4] has been largely used in this paper. This approach, in spite of the simplicity of the proof, is enormously powerful.

We have demonstrated that cylindrical distributions of currents can be managed analytically and generate pure 3-D magnetic multipoles. The general formulae for any order have been obtained; the specific formulae relative to dipoles and quadrupoles have been developed in detail. The dipole formulae correspond to rectangular dipoles. Nevertheless, we observe that since they are valid for any length we can obtain the magnetic field of a sector dipole as a sum of a very thin dipole–quadrupole distributed along the arc. The only inconvenience of this solution, which satisfies Maxwell's equations, is the long computing time.

In the solenoidal cases, coil and solenoid have been treated, with some caution, as a limit case of our formulae for $m = 0$.

The cylindrical models developed here are very useful for representing the magnetic elements of accelerators in simulation codes to study the effect of non-linearities on beam dynamics. Once the field behaviour of an element is known either by 3-D codes, or by magnetic measurement, it is possible to approximate the data with the function G_{m0}, by playing with the parameters R, Z_L to fit the shape, and I_c to fit the value. From there on the field is analytically determined up to any order, and this provides a wide flexibility in the codes.

A first application has been the study of the interaction regions of DAΦNE, the Frascati Φ-factory storage ring.[11,12] Owing to the beam-beam crossing angle, the beams pass off-axis in low-beta quadrupoles and solenoids. By representing the fields with our analytical formulae it has been possible to study the modification of the linear optics and of the on-axis compensation scheme. The effect of the pseudo-octupole present in the quadrupole fringing region[7,13] is automatically included.

Some examples of how the magnetic elements have been represented are shown in the following figures: Figure 12 refers to the permanent magnet quadrupole that will be installed in the DAΦNE low-beta region; the behaviour of the measured linear gradient is compared with the function G_{20} fitting it. The slight asymmetry of the data is due to a geometrical asymmetry of the quadrupole necessary to fit the detector space requirements. The two parameters which have been used to fit the data are $R = 0.08$ m and $Z_L = 0.10$ m.

Figure 13 represents the same curves for one of the normal conducting quadrupoles of the ring. In this case the data are symmetrical except for the measurement errors. $R = 0.10$ m and $Z_L = 0.15$ m have been used.

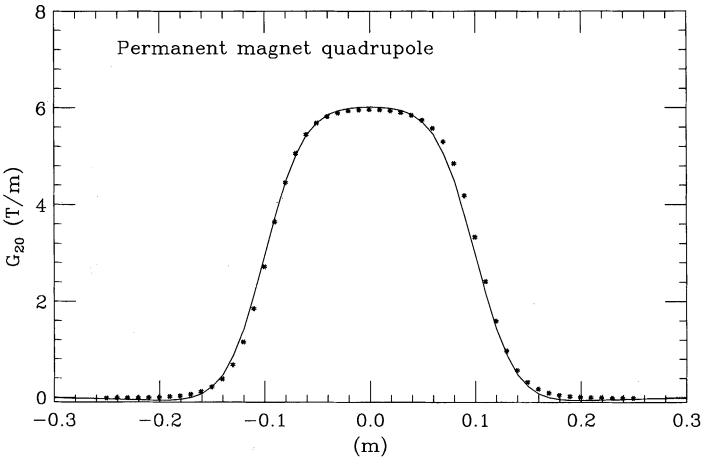

FIGURE 12: DAΦNE permanent magnet quadrupole - ****** measured linear gradient; —— function G_{20}.

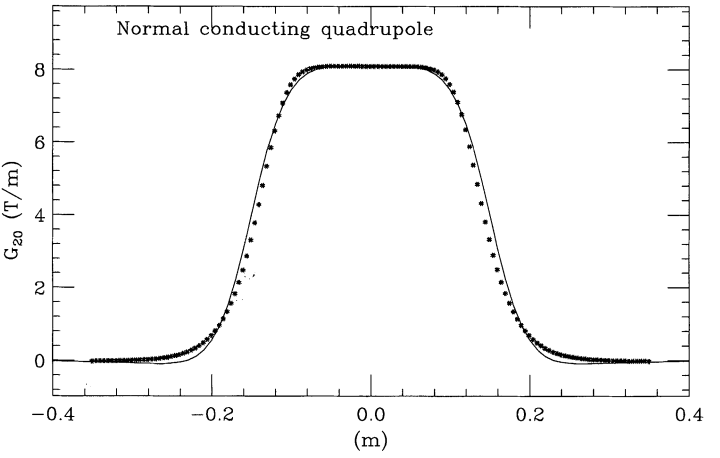

FIGURE 13: DAΦNE iron quadrupole - ****** measured linear gradient; —— function G_{20}.

In Figure 14 the longitudinal component of the magnetic field in one of the compensator solenoids is represented; the stars correspond to the field calculated with a 3-D magnetic code, the solid lines correspond to the field obtained with a combination of two cylindrical solenoids centred in the same position, which fit reasonably the bumps in the field behaviour. In fact the two function parameters are: $R_1 = 0.128$ m, $R_2 = 0.265$ m, $Z_{L1} = 0.41$ m, $Z_{L2} = 0.28$ m; $I_2 = -0.45\, I_1$.

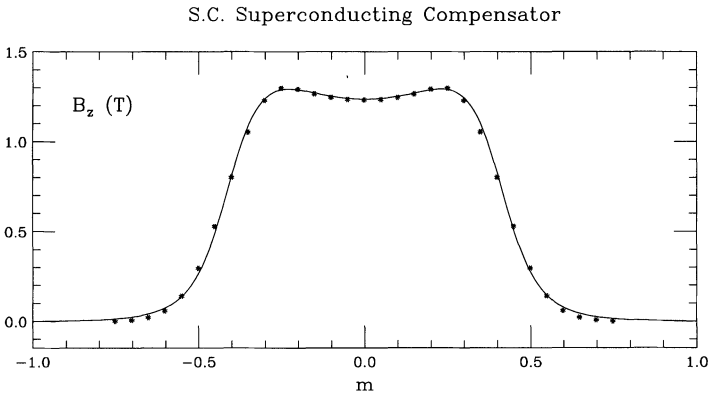

FIGURE 14: DAΦNE compensating solenoid - ****** 3-D code computed B_z; —— B_z obtained with the combination of two G_{20}.

Acknowledgements

The first author's interest about fringing fields was sparked after enlightening discussions with C. Iselin of CERN during the summer of 1993.

This work would not have been possible without initial research done by means of computer codes treating the field generated by fixed distributions of currents. It is a pleasure for the authors to thank C. Milardi for her collaboration in this phase of the work.

The authors are grateful to M. Preger and M. Serio of LNF, B. Zotter and W. Scandale of CERN and G. Fano of Bologna University for a careful reading of the paper.

APPENDIX A

A.1 Elaboration of Equation (40)

Let us consider the function:

$$g(r) = \frac{R - r\cos\theta}{\sqrt{[R^2 + r^2 - 2Rr\cos\theta + (Z-z)^2]^3}} \,. \tag{A.1}$$

Defining:

$$s = \sqrt{R^2 + r^2 - 2Rr\cos\theta + (Z-z)^2} \tag{A.2}$$

$$f(r) = R - \cos\theta \tag{A.3}$$

$$h(r) = r - R\cos\theta \tag{A.4}$$

we can simply write:

$$g(r) = \frac{f(r)}{s^3} \,. \tag{A.5}$$

Denoting by a prime the derivative with respect to r, we get:

$$f' = -\cos\theta \tag{A.6}$$

$$h' = 1 \tag{A.7}$$

$$s' = \frac{h}{s} \,. \tag{A.8}$$

From the above equations, putting $r = 0$ we obtain:

$$A(Z - z) = s(0) = \sqrt{R^2 + (Z - z)^2} \tag{A.9}$$

$$f(0) = R \tag{A.10}$$

$$g(0) = \frac{R}{A^3} \tag{A.11}$$

$$h(0) = -R\cos\theta \,. \tag{A.12}$$

By differentiating $g(r)$ m times, we get terms whose dependence on θ is proportional to $\cos^n\theta$ with n between 0 and m. If we look at the integration over θ of Equation (39) we already have a term $\cos m\theta$. The integrals to be performed have the form:

$$T(m, n) = \int_0^{2\pi} \cos m\theta \cos^n\theta d\theta \,. \tag{A.13}$$

Considering that:

$$\cos\theta = \frac{e^{i\theta} + e^{-i\theta}}{2} \tag{A.14}$$

and taking the n-th power of (A.14) the sum of the first and the last terms gives $\cos n\theta/2^{n-1}$. The other terms contain a lower integer multiple of θ. So we obtain:

$$T(m,n) = \frac{1}{2^{m-1}} \int_0^{2\pi} \cos m\theta \cos n\theta d\theta + \text{const} \int_0^{2\pi} \cos m\theta \cos(n-2)\theta d\theta + \cdots \tag{A.15}$$

$T(m,n)$ is different from 0 only if $m = n$:

$$T(m,m) = \frac{1}{2^{m-1}} \int_0^{2\pi} \cos^2 m\theta d\theta = \frac{\pi}{2^{m-1}} \tag{A.16}$$

$$\frac{\partial^m g}{\partial r^m} = \frac{a_m f h^m}{s^{2m+3}} + \frac{b_m f' h^{m-1}}{s^{2m+1}} \,. \tag{A.17}$$

The coefficient a_m is the product with alternating sign of the odd numbers starting from 1, namely:

$$a_m = (-1)^m \prod_{p=1}^{p=m} (2p+1) \,. \tag{A.18}$$

In the mathematical literature for simplicity the two following definitions are routinely used:

$$(2m+1)!! = \prod_{p=1}^{p=m} (2p+1) \tag{A.19}$$

$$(2m)!! = \prod_{p=1}^{p=m} (2p) \,. \tag{A.20}$$

As the function $p!!$ is not universally known, in the text we will use the equivalent formula:

$$(2m)!! = 2^m m! \tag{A.21}$$

$$(2m+1)!! = \frac{(2m+1)!}{(2m)!!} = \frac{(2m+1)!}{2^m m!} . \tag{A.22}$$

We can derive b_m by keeping separated the terms that are deduced from the derivation of f. We obtain therefore:

$$\begin{aligned}
\frac{\partial g}{\partial r} &= -\frac{3fh}{s^5} + \frac{f'}{s^3} \\
\frac{\partial^2 g}{\partial r^2} &= \left(\frac{15fh^2}{s^7} - \frac{3f'h}{s^5}\right) - \frac{3f'h}{s^5} \\
\frac{\partial^3 g}{\partial r^3} &= \left(-\frac{105fh^3}{s^9} + \frac{15f'h^2}{s^7}\right) + \frac{15f'h^2}{s^7} + \frac{15f'h^2}{s^7} .
\end{aligned} \tag{A.23}$$

Every differentiation adds a new term equal to the ones already obtained. Clearly after m derivations we find:

$$b_m = m a_{m-1} = m(-1)^{m-1}(2m-1)!! \tag{A.24}$$

and grouping the two terms:

$$\frac{\partial^m g}{\partial r^m} = (-1)^m h^{m-1} \left(\frac{(2m+1)!! fh}{s^{2m+3}} - \frac{m(2m-1)!! f'}{s^{2m+1}}\right) . \tag{A.25}$$

Substituting in the functions their value for $r = 0$, and using the definition (A.9) for $s(0)$ one obtains:

$$\left(\frac{\partial^m g}{\partial r^m}\right)_{r=0} = \cos^m \theta \left(\frac{(2m+1)!! R^{m+1}}{A^{2m+3}} - \frac{m(2m-1)!! R^{m-1}}{A^{2m+1}}\right) . \tag{A.26}$$

If we multiply (A.22) by $\cos m\theta$ and take into account Equations (A.16) and (A.22) we obtain for the integral over θ of Equation (A.39):

$$\int_0^{2\pi} \cos m\theta \left(\frac{\partial^m g}{\partial r^m}\right)_{r=0} d\theta = \frac{4\pi(2m-1)!R^{m-1}}{(m-1)!4^m}\left(\frac{(2m+1)R^2}{A^{2m+3}} - \frac{m}{A^{2m+1}}\right). \tag{A.27}$$

A.2 Integration on Z of G_{m0} (Z,z)

Let us now turn to the integration over Z of Equation (40). By using (27) it can be rewritten:

$$G_{m0}(Z,z) = \frac{\mu_0 I_c (2m-1)!R^{m-1}}{4^m(m-1)!}\int\left(\frac{(2m+1)R^2}{A^{2m+3}} - \frac{m}{A^{2m+1}}\right)dZ\,. \tag{A.28}$$

Recalling:

$$t = Z - z \tag{A.29}$$

$$A(t) = \sqrt{R^2 + t^2} \tag{A.30}$$

let us consider the integral:

$$I_m(t) = \int\left(\frac{(2m+1)R^2}{A^{2m+3}} - \frac{m}{A^{2m+1}}\right)dt\,. \tag{A.31}$$

The two integrals of (A.31) have the following form:

$$F_m = \int \frac{dt}{A^{2m+1}}\,. \tag{A.32}$$

Defining:

$$f_m(t) = \left(\frac{t}{A}\right)^m \tag{A.33}$$

the integral (A.32) can be written[14] as:

$$F_m = \frac{1}{R^{2m}}\sum_{k=0}^{m-1}\frac{(-1)^k f_{2k+1}(t)}{2k+1}\binom{m-1}{k}. \tag{A.34}$$

Applying Equation (A.34) the total integral in (A.28) becomes:

$$I_m(t) = \frac{1}{R^{2m}} \left[\sum_{k=0}^{m-1} \left(\frac{2m+1}{2k+1} \binom{m}{k} - \frac{m}{2k+1} \binom{m-1}{k} \right) \right.$$
$$\left. (-1)^k f_{2k+1} + (-1)^m f_{2m+1} \right] . \tag{A.35}$$

Each coefficient inside the sum, using well-known properties of binomial coefficients, can be written as:

$$\frac{(2m+1)}{(2k+1)} \binom{m}{k} - \frac{m}{2k+1} \binom{m-1}{k} = \frac{(m+k+1)}{(2k+1)} \binom{m}{k} \tag{A.36}$$

and therefore:

$$I_m(t) = \frac{1}{R^{2m}} \left(\sum_{k=0}^{m-1} (m+k+1) \binom{m}{k} (-1)^k \frac{f_{2k+1}}{2k+1} + (-1)^m f_{2m+1} \right) . \tag{A.37}$$

If $k = m$ the result of (A.36) is equal to 1. Therefore we can include the last term $(-1)^m f_m(t)$ of (A.35) inside the sum provided we extend it up to m and then:

$$I_m(t) = \frac{1}{R^{2m}} \sum_{k=0}^{m} (-1)^k \frac{m+k+1}{2k+1} \binom{m}{k} f_{2k+1}(t) \tag{A.38}$$

and:

$$G_{m0}(t) = \frac{\mu_0 I_c (2m-1)!}{4^m (m-1)! R^m} \sum_{k=0}^{m} (-1)^k \frac{m+k+1}{2k+1} \binom{m}{k} f_{2k+1}(t) . \tag{A.39}$$

APPENDIX B

B.1 Calculation of Derivatives of $f_h(t)$

Recalling the definitions (A.30) and (A.33):

$$A(t) = \sqrt{R^2 + t^2} \tag{B.1}$$

$$f_h = \left(\frac{t}{A}\right)^h \tag{B.2}$$

and by using the partial result:

$$\frac{\partial A}{\partial t} = \frac{t}{A} = f_1 \tag{B.3}$$

it is easy to deduce:

$$\frac{\partial f_h}{\partial t} = h\frac{R^2}{A^3} f_{h-1} \tag{B.4}$$

and differentiating again:

$$\frac{\partial^2 f_h}{\partial t^2} = \frac{1}{R^2}\left(\frac{h(h-1)R^6}{A^6} f_{h-2} - \frac{3hR^4}{A^4} f_h\right) . \tag{B.5}$$

In order to eliminate the powers A^6 and A^4 (B.2) suggests the replacement of R^2 by $(A^2 - t^2)$ obtaining:

$$R^4 = A^4 - 2A^2t^2 + t^4 \tag{B.6}$$

$$R^6 = A^6 - 3A^4t^2 + 3A^2t^4 - t^6 \tag{B.7}$$

and then:

$$\frac{\partial^2 f_h}{\partial t^2} = \frac{(h^2 - h) f_{h-2} - 3h^2 f_h + (3h^2 + 3h) f_{h+2} - (h^2 + 2h) f_{h+4}}{R^2} . \tag{B.8}$$

References

[1] S. Caspi, M. Helm and L.J. Laslett, *3-D Field Harmonics*, Lawrence Berkeley Laboratory Report 30313, March 1991.

[2] S. Caspi, M. Helm, L.J. Laslett and V.O. Brady, *An Approach to 3-D Magnetic Field Calculations Using Numerical and Differential Algebra Methods*, Lawrence Berkeley Laboratory Report 32624, July 1992.

[3] S. Caspi, M. Helm, and L.J. Laslett, *The Use of Harmonics in 3-D Magnetic Fields*, IEEE Trans. Magn. **30** (1994) 2419.

[4] G. Leleux, *Compléments sur la Physique des Accélérateurs*, Report Laboratoire National Saclay/86–101, March 1986.

[5] E. Regenstreif, Proc. Los Alamos Linac Conference (1966).

[6] R.L. Gluckstern, Brookhaven National Laboratory Report AADD 122 (1966).

[7] J. Le Duff, *Excitation of Non-Linear Resonances by the Fringing Field of the Insertion Quadrupoles in DORIS*, Report DESY H 72/2, June 1974.
[8] Wolfgang K.H. Panofsky and Melba Phillips, *Classical Electricity and Magnetism*, (Addison-Wesley, Reading, 1962).
[9] John D. Jackson, *Classical Electrodynamics*, (Wiley, New York, 1975), p. 173.
[10] E. Amaldi, *Fisica Sperimentale II*, (Club del Libro, Milano, 1950) p. 400.
[11] C. Biscari, *Low Beta Quadrupole Fringing Field on Off-Axis Trajectory*, AIP Conference Proceedings 344, (1994), pp. 88–93.
[12] M. Bassetti and C. Biscari, *Off-Axis Fields in DAΦNE Interaction Regions*, in preparation.
[13] P. Krejcik, *Nonlinear Quadrupole End-Field Effects in CERN Antiproton Accumulators*, Particle Accelerator Conference, (1987), Vol. 2, pp. 1278–1280.
[14] W. Gröbner and Nikolaus Hofreiter, *Unbestimmte Integrale* (Springer-Verlag, Berlin, 1957).